

# RSC Advances



This is an *Accepted Manuscript*, which has been through the Royal Society of Chemistry peer review process and has been accepted for publication.

*Accepted Manuscripts* are published online shortly after acceptance, before technical editing, formatting and proof reading. Using this free service, authors can make their results available to the community, in citable form, before we publish the edited article. This *Accepted Manuscript* will be replaced by the edited, formatted and paginated article as soon as this is available.

You can find more information about *Accepted Manuscripts* in the [Information for Authors](#).

Please note that technical editing may introduce minor changes to the text and/or graphics, which may alter content. The journal's standard [Terms & Conditions](#) and the [Ethical guidelines](#) still apply. In no event shall the Royal Society of Chemistry be held responsible for any errors or omissions in this *Accepted Manuscript* or any consequences arising from the use of any information it contains.

Cite this: DOI: 10.1039/c0xx00000x

www.rsc.org/xxxxxx

## ARTICLE TYPE

## Polyethyleneimine templated synthesis of hierarchical SAPO-34 zeolites with uniform mesopores

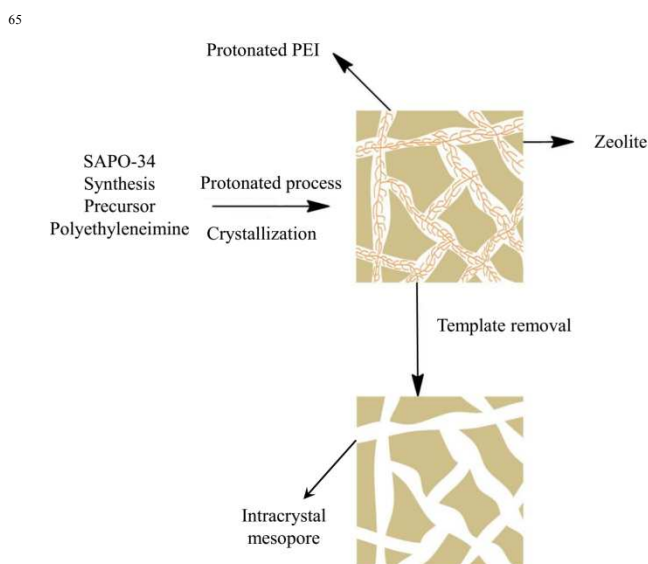
Fei Wang,<sup>a</sup> Long Sun,<sup>a</sup> Chuanling Chen,<sup>a</sup> Zhen Chen,<sup>a</sup> Zhenwei Zhang,<sup>b</sup> Guohui Wei<sup>c</sup> and Xingmao Jiang<sup>\*a,c</sup><sup>5</sup> Received (in XXX, XXX) Xth XXXXXXXXX 20XX, Accepted Xth XXXXXXXXX 20XX  
DOI: 10.1039/b000000x

SAPO-34 zeolites with uniform mesopores have been successfully synthesized using polyethyleneimine (PEI) dendrimer as co-temple through conventional hydrothermal synthesis for microporous crystalline SAPO-34. This series of SAPO-34 possesses higher BET specific surface area (as high as 560 m<sup>2</sup>g<sup>-1</sup>) and larger mesoporous volume (as large as 0.27 cm<sup>3</sup> g<sup>-1</sup>). The size and volume for the mesopores can be adjusted by the molecular weight and the amount of the PEI added. The hierarchical SAPO-34 would be potential industrial catalysts for methanol-to-olefin (MTO) and methanol-to-propylene (MTP) conversions.

Owing to their high surface area, large pore volume, uniform microporous channels, and excellent thermal and hydrothermal stabilities, zeolites especially microporous crystalline aluminophosphates (AlPOs), silicoaluminophosphates (SAPOs) and metal-substituted AlPOs (MAPOs) are currently regarded as the most useful zeolitic catalysts for industrial processes including oil refining and manufacture of fine chemicals.<sup>1-5</sup> For example, SAPO-34 zeolite has been shown as an efficient industrial catalyst for MTO and MTP conversions.<sup>5</sup> However, the micropores are easy to be plugged by coking, which tends to deactivate rapidly the catalysts. With the discovery of surfactant-templated synthesis of mesoporous silicate based molecular sieves,<sup>6</sup> which offer fast mass transfer along with size and shape selectivity, developing a new class of hierarchical mesoporous zeolites becomes a focus of interest for catalyst researchers.<sup>7-10</sup> Mesoporous SAPO-34 zeolites exhibiting excellent catalytic performance have received increasing attention and have been successfully synthesized using various surfactants.<sup>11-14</sup> For example, Yu et al. reported that hierarchical porous SAPO-34 catalysts were successfully synthesized using organosilane surfactant, ([3-(trimethoxysilyl)propyl]-octadecyldimethylammonium chloride) as the mesopore template by direct hydrothermal crystallization.<sup>13</sup> However, use of expensive surfactants as the templates not only increases the cost of zeolites, but also lacks good control of the size and volume of the mesopores.

In recent years, significant progress has been made in controlled synthesis of zeolites using various polymers.<sup>15,16</sup> Miyake et al. reported that ordered mesoporous silicoaluminophosphates were synthesized using PEO<sub>106</sub>PPO<sub>70</sub>PEO<sub>106</sub> triblock copolymer.<sup>17</sup>

Compared with the block polymers, polyethyleneimine (PEI) is a dendrimer with a repeating unit composed of an amine group and two-carbon chain, and that is inexpensive and readily available in several molecular weights,<sup>18</sup> which differs far from currently used meso-templates. Previous work<sup>19,20</sup> revealed that PEI molecules are highly coiled at basic conditions (pH > 9), and while at acidic conditions (pH < 7) are elongated. Silylated polyethyleneimine has been successfully applied as the silicon source and the meso-<sup>55</sup> template to synthesize MFI type zeolites with uniform intracrystalline mesopores, and it was believed that the silylation is essential for effective incorporation of the polymer into a growing zeolite matrix and formation of the mesostructure.<sup>21</sup> However, silylation of the polymers makes the synthesis of mesoporous zeolites complicated and expensive. Therefore, synthesizing mesoporous zeolites using non-silylated PEI directly as the template becomes an interesting topic and challenging problem.



Scheme 1 Proposed synthesis mechanism for mesoporous SAPO-34.

Herein, we report a novel strategy using PEI as the mesopore directing agent to synthesize SAPO-34 with uniform mesopores. Scheme 1 illustrates our synthetic route for templating uniform mesopores within a zeolite matrix. Triethylamine (TEA) and PEI

(Mw=70000) were selected as the directing agents for micropores and mesopores, respectively. Phosphoric acid was involved during the formation of zeolite gel to protonate the amine groups of PEI. In this scheme, the protonated PEI polymer is used as a porogen for the formation of intracrystal mesopores. The protonated PEI chains are elongated at low pH and well connected through hydrogen bonding and van der Waals forces interactions between ethyleneimine segments. The PEI molecules interact with oxide species in the silica–alumina- phosphoric acid sol–gel system through molecular self-assembly based on non-covalent bonds such as hydrogen bonding and van der Waals forces. During the hydrothermal process, the incorporated PEI molecules segregate from the zeolite matrix, forming an interconnected continuous crystalline SAPO-34 phase and organic amine liquid crystal phase by molecular self-assembly and zeolite crystallization. After crystallization at 200 °C for 50 h, particulate hydrothermal products were filtered, washed and calcined to remove the TEA and PEI templates, and SAPO-34 molecular sieve with mesoporous structures was obtained, which was denoted as PEI-SAPO-34. In order to investigate the impact of the molecular weight and amount of the PEI on the mesostructure of PEI-SAPO-34, PEI templates of two different molecular weights (Mw=1800 and 10000) were studied as well. Furthermore, the above strategy was applied for preparation of ZSM-5 and LTL molecular sieves which requires basic synthesis conditions. For comparison, conventional SAPO-34 was also synthesized without addition of the PEI templates.

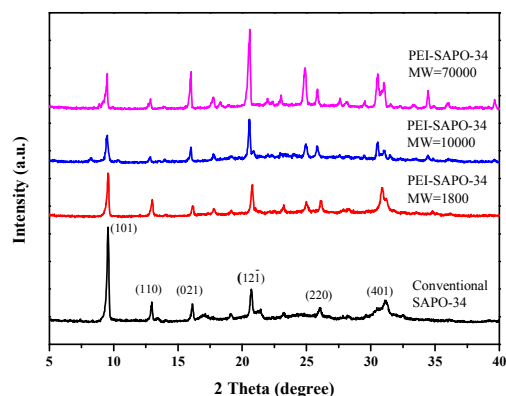


Fig. 1 X-ray diffraction patterns of SAPO-34 and PEI-SAPO-34 zeolites.

As shown in Fig. 1, in comparison with the conventional SAPO-34, XRD patterns of the as-synthesized samples show well-resolved peaks in the range of 5–40° (Fig. 1), which are in good agreement with that of SAPO-34 rhombohedral structure (JCPDS 01-087-1527) as indicated by diffraction peak at  $2\theta = 9.4, 12.9, 16.15, 20.5, 26.1$  and  $30.5^\circ$  without any presence of impurity phase, which were indexed to (101), (110), (021), (12 $\bar{1}$ ), (220) and (401) planes of SAPO-34, respectively.<sup>22</sup> However, the corresponding  $I_{(101)}/I_{(12\bar{1})}$  ratio obviously decreased from 3.14 to 0.47 with increasing the molecular weight of the PEI, implying preferential crystal growth along the (12 $\bar{1}$ ) orientation in the presence of PEI. Compared with conventional SAPO-34, this result demonstrated that addition of PEI made the pore structure

of SAPO-34 orientated. The thermal chemical and physical properties of PEI-SAPO-34 were measured by thermal gravimetric analysis (TGA) (Fig. S1, ESI†). The TGA result shows three weight losses in the range of 50–800 °C. The first weight loss of ~5 % in the low temperature range of 50–100 °C is attributed to the desorption of CO<sub>2</sub> and moisture from the sample. In the second (300–500 °C) and the third stages (500–650 °C), weight losses of ~6 % and ~7 % respectively occur due to the decomposition of triethylamine and PEI. At above 650 °C, the PEI was completely decomposed and removed as volatiles, which agrees well with the literature.<sup>23</sup>

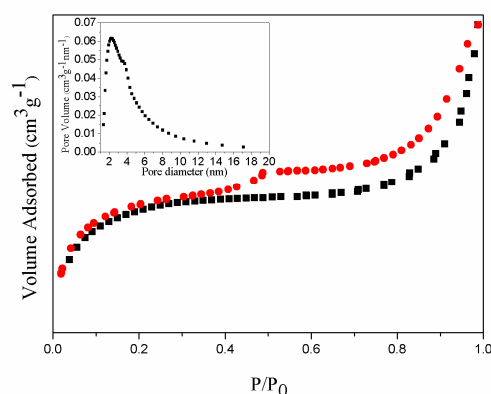


Fig. 2 Nitrogen adsorption/desorption isotherms for PEI-SAPO-34 prepared in the presence of PEI (Mw=70000). Inset is the BJH pore size distribution.

Fig. 2 provides the nitrogen adsorption/desorption isotherm for as-synthesized PEI-SAPO-34 (Mw=70000). Compared to the conventional SAPO-34, the PEI-SAPO-34 shows a type-IV adsorption/desorption isotherm, which presents a distinct increase of adsorption quantity in the region  $0.4 < P/P_0 < 0.9$  owing to the capillary condensation in the mesopores. The inset of Fig. 2 shows the BJH mesopore size distribution for PEI-SAPO-34. It can be seen that the PEI-SAPO-34 possessed narrow Barrett-Joyner-Halenda (BJH) pore size distribution and its average pore size is centered between 2.0 and 3.0 nm. The BET specific surface area and mesopore volume of PEI-SAPO-34 were measured to be  $560 \text{ m}^2 \text{ g}^{-1}$  and  $0.27 \text{ cm}^3 \text{ g}^{-1}$ , respectively.

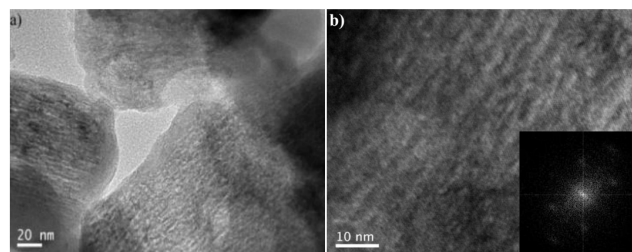


Fig. 3 TEM images of mesoporous PEI-SAPO-34 (Mw=70000): a) Low magnification; b) High magnification. Inset: fast Fourier transform (FFT) diffractogram of PEI-SAPO-34.

The presence of intracrystal mesopores was also evidenced by TEM technique. Fig. 3 shows the TEM images of PEI-SAPO-34 (Mw=70000). In the lower-magnified image (Fig. 3a), orientated uniform mesopores were found. Furthermore, the pores can be

observed more clearly in the higher-magnified image (Fig. 3b), and the sample shows a regular array of uniform pore characteristics of SAPO-34 type channels in the range from 2.0 to 3.0 nm, which is consistent with the result of BJH measurement. FFT pattern (Fig. 3b, insert) of the PEI-SAPO-34 sample shows spot pattern might be due to short range order of mesoporous phase, confirming that PEI-SAPO-34 is comprised of single crystals rather than random aggregations of nanocrystals. Based on the results of XRD, TEM and pore structure characterization, PEI-SAPO-34 with uniform mesopores has been successfully synthesized by self-assembly using protonated branched PEI template.

Table 1 Pore structure properties of different as-synthesized samples.

Sample	$S_{\text{BET}}$ ( $\text{m}^2 \text{g}^{-1}$ )	$V_{\text{meso}}$ ( $\text{cm}^3 \text{g}^{-1}$ )	$D$ (nm)	$V_{\text{micro}}$ ( $\text{cm}^3 \text{g}^{-1}$ )
PEI-SAPO-34 ( $M_w=1800$ )	410	0.11	1.7	0.112
PEI-SAPO-34 ( $M_w=10000$ )	485	0.17	1.9	0.108
PEI-SAPO-34 ( $M_w=70000$ )	560	0.27	2.2	0.117
ZSM-5 ( $M_w=70000$ )	350	n.a.	n.a.	0.103
LTL ( $M_w=70000$ )	320	n.a.	n.a.	0.094

$S_{\text{BET}}$  is BET specific surface area,  $V_{\text{meso}}$  mesoporous pore volume,  $V_{\text{micro}}$  microporous pore volume, and  $D$  is mesoporous pore size.

Additionally, we investigated effect of the molecular weight and amount of the PEI added on the pore structures of PEI-SAPO-34. As shown in Table 1, the BET specific surface area, mesopore volume and mesopore size increased gradually from 410 to 560  $\text{m}^2 \text{g}^{-1}$ , 0.11 to 0.27  $\text{cm}^3 \text{g}^{-1}$  and 1.7 to 2.2 nm respectively with the molecular weight of PEI ranging from 1800 to 70000, while the micropore volume keeps almost constant (about 1.11  $\text{cm}^3 \text{g}^{-1}$ ) under same addition of triethylamine. The degree of branched polymerization becomes enhanced with the increase of PEI molecular weight, resulting in enlargement of the mesopore sizes, which was similar with the results reported by Wang et al.<sup>21</sup> With the addition of the PEI increasing from 0.5 g to 2 g, both mesopore volume and mesoporous pore size also increased (Fig. S2 and Table S1, ESI†). So it can be deduced that the mesopore volume and mesoporous pore of synthesized SAPO-34 zeolite can be controlled through adjusting the molecular weight and the amount of the PEI. Moreover, the effect of the pH value of the precursor system on the formation of the mesoporous zeolite was also investigated. Efforts were made to prepare ZSM-5 and LTL by using PEI as the mesoporous directing agent. The pH values of the initial gel of ZSM-5 and LTL were 11.87 and 13.05 respectively, which was consistent with previous reports.<sup>24,25</sup> As shown in Table 1, there is no detectable mesoporous structure for ZSM-5 and LTL zeolites under same addition of PEI. These results demonstrated that when the pH value was higher than 11, polyethylenimine molecules are easily coiled into big aggregates, minimizing the interaction between PEI aggregates with zeolite precursor molecules and reducing chance of encapsulation of PEI aggregates in zeolite matrix. In contrast, as the pH value of the precursor for SAPO-34 synthesis was only 6.78, the PEI chains

extended under acid conditions and SAPO-34 with uniform mesopores were formed along the interconnecting main linear chains of PEI. Hence, the technique using PEI as the mesopore directing agent should be general and promising for synthesis of those zeolites, which requires acidic or less basic conditions. The zeolites include silicoaluminophosphate, aluminophosphate- and heteroatom-containing aluminophosphate zeolites, such as SAPO-11, SAPO-43, APO-11, Co-APO-11, Mg-SAPO-46 and so on. The preparation of these zeolites is still in progress in this lab. In summary, we have demonstrated a novel synthesis process for hierarchical SAPO-34 zeolites with uniform mesopores using a cationic polymer (polyethylenimine) as the mesopore directing agent. The method provides much flexibility in the control of mesopore size and pore volume. Compared to current methods for mesoporous SAPO-34, this technique excels in offering an uniform mesoporous structure, a large mesoporous volume (0.27  $\text{cm}^3 \text{g}^{-1}$ ) and a high BET specific surface area (560  $\text{m}^2 \text{g}^{-1}$ ), which would be beneficial for mass transport of reactants and catalytic reaction products, thereby inhibiting the catalyst from coking and deactivation. Taking all of these features into account, it is believable that this synthesis strategy for synthesizing aluminophosphate-based zeolites will be of great importance for industrial production in the future. In particular, mesoporous SAPO-34 is a promising commercial catalyst for MTO and MTP conversions.

## Acknowledgements

This work was financially supported by the National Natural Science Foundation of China (Nos. 21373034, 21201140), the Specially Hired Professorship-funding of Jiangsu Province (No. SCZ1211400001), Key University Science Research Project of Jiangsu Province (No. 13KJA530001) and the Start-up Funds from Changzhou University of Jiangsu Province, Jiangsu key Laboratory of Advanced Catalytic Material and Technology and PAPD of Jiangsu Higher Education Institutions.

## Notes and references

- <sup>a</sup> Key Laboratory of Advanced Catalytic Material and Technology, Changzhou University, Changzhou 213164, PR China. Fax: +86-519-8633-0251; Tel: +86-519-8633-0253
- <sup>b</sup> State Key Laboratory of Materials-Oriented Chemical Engineering, College of Chemistry and Chemical Engineering, Nanjing University of Technology, Nanjing 210009, PR China.
- <sup>c</sup> Changzhou Yingzhong Nano Technology Co., Ltd., Changzhou 213164, PR China.
- †Electronic Supplementary Information (ESI) available: [details of any supplementary information available should be included here]. See DOI: 10.1039/c000000x/
- S. T. Wilson, B. M. Lok, C. A. Messian, T. R. Cannanand and E. M. Flanigen, *J. Am. Chem. Soc.*, 1982, **104**, 1146–1147.
- H. O. Pastore, S. Coluccia and L. Marchese, *Annu. Rev. Mater. Res.*, 2005, **35**, 351–395.
- J. Yu and R. Xu, *Acc. Chem. Res.*, 2003, **36**, 481–490.
- H. Oikawa, Y. Shibata, K. Inazu, Y. Iwase, K. Murai, S. Hyodo, G. Kobayashi and T. Baba, *Appl. Catal. A*, 2006, **312**, 181–185.
- Y. Y. Jin, Q. Sun, G. D. Qi, C. G. Yang, J. Xu, F. Chen, X. J. Meng, F. Deng and F. S. Xiao, *Angew. Chem., Int. Ed.*, 2013, **52**, 9172–9175.
- J. S. Beck, J. C. Vartuli, W. J. Riith, M. E. Leonowicz, C. T. Kresge, K. D. Schmitt, C. T. W. Chu, D. H. Olson and E. W. Sheppard, *J. Am. Chem. Soc.*, 1992, **114**, 10834–10843.



- 7 F. J. Liu, T. Willhammar, L. Wang, L. F. Zhu, Q. Sun, X. J. Meng, W. Carrillo-Cabrera, X. D. Zou and F. S. Xiao, *J. Am. Chem. Soc.*, 2012, **134**, 4557–4560.
- 8 K. Na, M. Choi and R. Ryoo, *Micropor. Mesopor. Mat.*, 2013, **166**, 3–19.
- 9 W. Q. Fu, L. Zhang, T. D. Tang, Q. P. Ke, S. Wang, J. B. Hu, G. Y. Fang, J. X. Li and F. S. Xiao, *J. Am. Chem. Soc.*, 2011, **133**, 15346–15349.
- 10 M. Reichinger, W. Schmidt, V. V. Narkhede, W. P. Zhang, H. Gies and W. Grunert, *Micropor. Mesopor. Mat.*, 2012, **164**, 21–31.
- 11 A. K. Singh, R. Yadav and A. Sakthivel, *Micropor. Mesopor. Mat.*, 2013, **181**, 166–174.
- 12 Y. L. Liu, L. Z. Wang, J. L. Zhang, L. J. Chen and H. S. Xu, *Micropor. Mesopor. Mat.*, 2011, **145**, 150–156.
- 13 Q. M. Sun, N. Wang, D. Y. Xi, M. Yang and J. H. Yu, *Chem. Commun.*, 2014, **50**, 6502–6505.
- 14 J. Zhu, Y. Cui, Y. Wang and F. Wei, *Chem. Commun.*, 2009, **22**, 3282–3284.
- 15 H. B. Zhu, Z. C. Liu, D. J. Kong, Y. D. Wang and Z. K. Xie, *J. Phys. Chem. C*, 2008, **112**, 17257–17264.
- 16 J. F. Yao, Y. Huang and H. T. Wang, *J. Mater. Chem.*, 2010, **20**, 9827–9831.
- 17 S. Tanakaa, R. Fukui and Y. Miyake, *Mater. Lett.*, 2013, **92**, 259–262.
- 18 B. L. Rivas and K. E. Geckeler, *Adv. Polym. Sci.*, 1992, **102**, 171–188.
- 19 C. K. Choudhury and S. Roy, *Soft Matter*, 2013, **9**, 2269–2281.
- 20 Z. W. Zhang, G. Zhang, L. He, L. Sun, X. M. Jiang and Z. Yu, *CrystEngComm.*, 2014, **16**, 3478–3482.
- 21 H. Wang and T. J. Pinnavaia, *Angew. Chem., Int. Ed.*, 2006, **45**, 7603–7606.
- 22 S. Aghamohammadi, M. Haghighi and M. Chorghand, *Mater. Res. Bull.*, 2014, **50**, 462–475.
- 23 X. C. Xu, C. S. Song, J. M. Andrésen, B. G. Miller and A. W. Scaroni, *Micropor. Mesopor. Mat.*, 2003, **62**, 29–45.
- 24 H. Feng, C. Y. Li and H. H. Shan, *App. Clay Sci.*, 2009, **42**, 439–445.
- 25 P. N. Joshi, N. E. Jacob and V. P. Shiralkar, *J. Phys. Chem.*, 1995, **99**, 4225–4229.